Identification of Cr species at the aqueous solution–hematite interface after Cr(VI)–Cr(III) reduction using GI-XAFS and Cr L-edge NEXAFS

Daniel Grolimund,[a]* **Thomas P. Trainor,**[a] **Jeffrey P. Fitts,**[a] **Tom Kendelewicz,**[a] **Ping Liu,**[a] **Scott A. Chambers**[c] **and Gordon E. Brown, Jr.**[a,b]

[a]*Stanford University, Geological & Environmental Sciences, Stanford, CA 94305-2115, USA,* [b]*Stanford Synchrotron Radiation Laboratory, SLAC, Stanford, CA 94309, USA,* [c]*Pacific Northwest National Laboratory, EMSL, Richland, WA 99352, USA. Email:daniel@pangea.stanford.edu*

Surface-mediated redox processes and sorption reactions occurring at the solid-liquid interface are of importance to a broad variety of environmental and industrial pollution or corrosion/passivation problems. A more fundamental under-standing of the mechanisms of these reactions is required in order to increase our ability to predict interfacial phenomena. In this study, gazing-incidence XAFS (GI-XAFS) and near-edge XAFS (both L- and K-edge NEXAFS) techniques were used to inves-tigate the chemical and structural characteristics of interfacial Cr(III) and Cr(VI) species on a molecular level. In particular, products of postulated electron transfer reactions between Cr(VI) and Fe(II) at the oxide-solution interface were investigated. Both techniques confirmed the reduction of Cr(VI) to Cr(III) mediated by a partially reduced hematite (0001) surface. The observed local structure of the interfacial chromium species emphasizes the need for an improved, molecular-level conceptualization of reactions occurring at the solid-solution interface.

Keywords: Grazing-incidence XAFS, molecular adsorption, electron transfer reaction (redox), chromium, single crystal hematite, hematite-aqueous solution interface

1. Introduction

In natural systems, the mobility as well as the potential hazard óf contaminants is controlled to a notable extent by their affinity for solid phases and, in the case of redox sensitive pollutants, by their oxidation state (Stumm & Morgan, 1996). Consequently, physicochemical reactions occurring at the solid-liquid interface, such as surface complexation or electron transfer reactions, are of central importance to a broad variety of environmentally relevant phenomena including the dispersal of pollutants in the subsurface zone, residence times of contaminants in surface waters, waste water treatment, and bioavailability of plant nutrients. In addition, sorption and surface redox processes are important in a number of industrial areas, including heterogeneous catalysis and corrosion/passivation of metal surfaces. The identification of reaction products is required to develop a molecular-level understanding of the mechanisms of such interfacial reactions. Resulting concepts would lead to an improved ability to predict the reactivity of different interfacial systems.

In this study we have used Cr K-edge GI-XAFS and Cr L-edge NEXAFS spectroscopy to investigate the types of surfaces complexes formed when aqueous Cr(VI) and Cr(III) react, respectively, with reduced (containing Fe(II)) and unreduced single crystal (0001) hematite surfaces. In the 6^+ form, aqueous Cr is both mobile and toxic to organisms, whereas in the 3^+ form, Cr is relatively insoluble and is less mobile and less toxic than Cr(VI). Thus, a knowledge of the speciation of Cr and the processes responsible for its transformation from Cr(VI) to Cr(III) is essential for predicting its potential impact as an environmental pollutant. A number of previous studies have shown that Cr(VI) is readily reduced in natural environments by interactions with minerals containing Fe(II) (e.g., Peterson et al., 1997a). However, it has also been shown in model systems that the surfaces of Fe(II)-containing oxides and hydroxides can become passivated as a result of Fe(III) oxyhydroxide formation (e.g., Peterson et al., 1997b; Kendelewicz et al., 1998). In this paper, we extend this earlier work to reduced hematite surfaces and examine the reaction of aqueous Cr(VI) with synthetic, near atomically smooth (0001) single crystal hematite surfaces. Our main objective is to provide additional insights about the mechanism of the Cr(VI) → Cr(III) redox reaction, including the nature of reaction products formed at the hematite surface.

2. Materials and methods

Thin (~350 Å) synthetic single crystal hematite (α-Fe_2O_3) samples were grown on oriented sapphire substrates by multiple beam epitaxy, resulting in atomically smooth (2-5 Å rms roughness) hematite (0001) surfaces (Kim et al., 1997). Partially reduced surfaces were produced by annealing at ~500°C in vacuum. The partially reduced hematite was exposed to a Cr(VI)-containing solution (5mM Na_2CrO_4, pH 6.0, 0.1M $NaNO_3$) in a N_2 atmosphere and immediately transferred to a UHV chamber for Cr L-edge NEXAFS data collection. Subsequently, the same sample was investigated using GI-XAFS under ambient conditions. In addition, unreduced thin-film hematite was exposed to a Cr(III) solution (10^{-5} M $Cr(NO_3)_3$, pH 4.8) in a N_2 atmosphere and analyzed by GI-XAFS under ambient conditions. Experimental conditions (e.g., pH, total Cr concentration) were chosen to avoid the formation of multinuclear Cr complexes or supersaturation of Cr species in solution with respect to known hydroxides, carbonates, or basic salts (e.g., Smith & Martell, 1976). X-ray photoelectron spectroscopy (XPS) was used to check for surface cleanliness prior to the experiment and to estimate surface coverage after reaction. In addition to Fe and O, only adventitious carbon (<30 atoms/nm^2) was detected. The observed Cr surface coverage was below 0.1 monolayer for the unreduced hematite while the partially reduced hematite sample yield a coverage of ~0.3 monolayer.

GI-XAFS/NEXAFS experiments were performed at SSRL (3GeV and 60-100mA) on beamlines 6-2 and 10-1. GI-XAFS data were collected using the SSRL grazing-incidence apparatus in the specular geometry with the incident angle set slightly below the critical angle of the hematite substrate at ~6 keV (~0.2°). GI-XAFS data analysis was performed using EXAFSPAK (George & Pickering, 1995), and k^3-weighted EXAFS were fit over a k-range of approximately 3-11 Å^{-1}. Phase and amplitude functions were calculated with FEFF7 (Rehr et al., 1992) and verified by comparison with model mineral compounds. The accuracy of the optimized parameters can be estimated based on fits of crystalline model compounds (first shell: N±15% and R±0.03Å; more distant shells: N±30% and R±0.07Å). The Debye-Waller term (σ^2) for each shell was estimated based on fits of both model compounds and single-

shell backtransforms and was kept fixed during the final optimization procedure.

3. Results and Discussion

3.1 Oxidation State and Coordination

Cr K-edge XAFS as well as Cr L-edge NEXAFS have been shown to be sensitive to the presence of different chromium oxidation states, Cr(VI) vs. Cr(III), in a mixed Cr(VI)-Cr(III) sample (e.g., Peterson et al., 1997b; Kendelewicz et al., 1998). Fig. 1a shows the Cr L-edge NEXAFS spectrum for Cr on a partially reduced hematite surface after exposure to a Cr(VI)-containing solution, while the corresponding Cr K-edge XAFS spectrum (near edge) is depicted in Fig. 1b. Metal L-edge spectroscopy is sensitive to oxidation state and geometry of the first coordination shell. The spectrum of a mixed system can be interpreted as a superposition of different individual spectra of isolated components and can therefore be resolved by comparison with suitable standards. As apparent from Fig. 1a, the L-edge spectrum of the sorption sample reveals features characteristic of both Cr(III) (cf. chromite) and Cr(VI) species (cf. crocoite) indicating that both oxidation states of chromium are simultaneously present at the hematite-solution interface in a ratio of ~25% Cr(III)-75% Cr(VI). The observed Cr(III) is the result of electron transfer reactions involving the oxidation of three Fe(II) in the partially reduced hematite to produce one Cr(III) at the hematite-aqueous solution interface. We also carried out a Cr K-edge NEXAFS analysis of the same sample after it had been analyzed by XPS, and the result is shown in Fig. 1b. The intensity of the Cr(VI) pre-edge feature, indicated by the arrow, suggests ~80% Cr(III) and ~20% Cr(VI) based on the calibration spectra of Peterson et al. (1996). The apparent difference between these two experiments is most likely due to further reduction of Cr(VI) on the partially reduced hematite (0001) surface during XPS analysis, which involved the use of an electron flood gun. Thus the Cr(VI):Cr(III) ratio from the L-edge spectrum is most reliable for our hematite samples. The simultaneous presence of both oxidation states at the interface even after extended exposure times points towards a limited reducing capacity which is depleted during the course of the experiment.
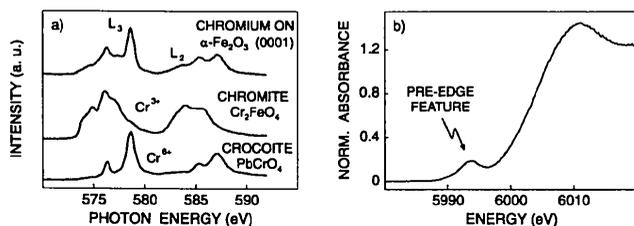
Figure 1

a) Normalized Cr L-edge NEXAFS spectra of a Cr(VI)-exposed, partially reduced hematite sample compared to Cr(VI) and Cr(III) model compounds. b) Corresponding Cr K-edge NEXAFS spectrum.

3.2 Hypothetical Sorption Complexes

Generally, surface complexation models postulate different coordination environments of isolated surface species without direct molecular-level knowledge of the types of surface complexes present (e.g., Dzombak & Morel, 1990). Several hypothetical surface complexes are depicted in Fig. 2 (top row), assuming a bulk terminated hematite (0001) surface. In addition,

Fig. 2 (bottom row) shows FEFF7-calculated Fourier transforms (FT) based on the postulated local structure of the surface complex, considering the well-defined orientation of the single crystal surface parallel to the E-vector. The polarization dependence of the K-edges gives higher effective coordination numbers for metal second neighbors that reside along the direction of the polarization vector (Citrin, 1985). This results in more pronounced features for surface complexes with a local environment of high symmetry. This phenomenon becomes most apparent in the case of mono-dentate and bi-dentate complexes, where nearest-neighbor features are diminished due to their perpendicular bond orientation relative to the E-vector.
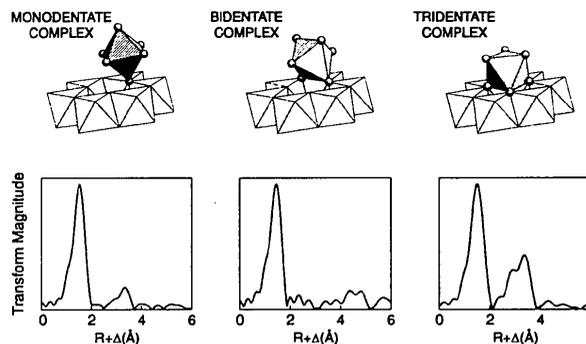
Figure 2

Top: Local geometric structure of hypothetical Cr(III) surface species. *Bottom*: Corresponding Fourier transforms (calculated).

3.3 Cr(III) Sorption on Single Crystal Hematite

Fig. 3 depicts the EXAFS spectra and resulting Fourier transforms of an unreduced hematite (0001) surface exposed to a Cr(III)-containing solution (Fig. 3, top) and a partially reduced sample exposed to aqueous Cr(VI) (Fig. 3, bottom). Despite the different reaction pathways, the least-squares fitting results in a similar local structure of the observed Cr surface species for both samples except for the presence of a ^{IV}Cr(VI)-O correlation for the partially reduced sample. The first FT feature is due to Cr-O correlations while the second FT feature is most likely due to Cr-Cr correlations. There is also evidence for a more distant (~3.5Å) metal-metal shell (Cr-Fe or Cr-Cr), which is difficult to resolve unambiguously. This third shell is best fit by a Cr-Fe correlation, and could be evidence for direct bonding of Cr(III) to the hematite surface. It is important to note that the GI-XAFS spectra taken with the E-vector parallel to the hematite surface should be relatively insensitive to Cr-metal correlations perpendicular to the hematite surface. GI-XAFS spectra taken with the E-vector perpendicular to the hematite (0001) surface are needed to confirm the presence of Cr-Fe$_{surface}$ correlations. None of the hypothetical complexes depicted in Fig. 2 is consistent with the local structure obtained in the GI-XAFS analysis. Consequently, we propose a multinuclear surface complex rather than a mononuclear complex, which is often assumed in surface complexation modeling (e.g., Dzombak and Morel, 1990). The observed metal-metal distance of ~3.0 Å is consistent with edge sharing metal-oxide (MeO$_6$) octahedra with either Fe or Cr as the central metal atom (Charlet & Manceau, 1992). Based on the fitted number of second-shell metal neighbors (~2), the Cr-metal clusters are limited in size or they are arranged in a disordered fashion. The lack of more pronounced next-nearest neighbor metal shell features is consistent with this finding and further emphasizes the limited size of the proposed "two-dimensional" multinuclear species.

The identity of the different metal backscatterer correlations can not be resolved unambiguously due to the similarity of the Cr and Fe phase shift and amplitude functions, respectively. Nevertheless, the GI-XAFS information provides relatively restrictive geometrical constraints due to the polarized nature of the spectra. Multinuclear Cr complexes, in particular dimers and trimers sorbed in a two-dimensional fashion to the atomically flat hematite (0001) surface, satisfy the observed spectra. The more distant metal-metal shell at 3.5Å is consistent with Fe backscatterers from the hematite surface arranged in a somewhat disordered fashion.
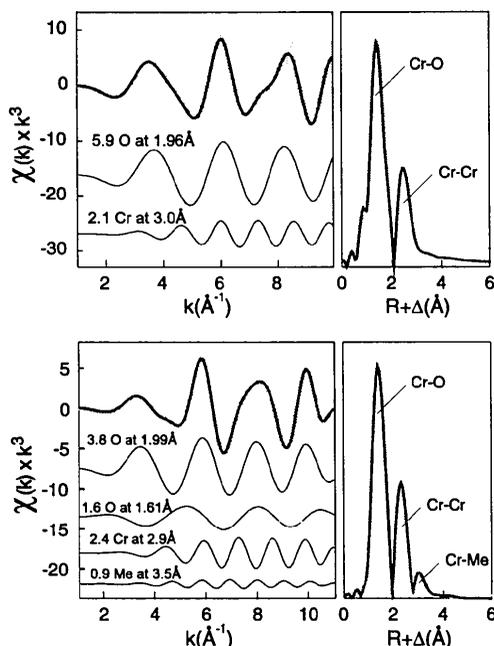
Figure 3

Grazing-incidence Cr K-edge XAFS data (grey) of chromium sorbed on α-Fe$_2$O$_3$ single crystals (0001). *Top*: Unreduced hematite (0001) reacted with Cr(III). *Bottom*: Partially reduced hematite exposed to Cr(VI). Least squares fits of the EXAFS including shell-by-shell deconvolution and Fourier transforms uncorrected for phase shift are shown.

Additional evidence for a true sorption complex comes from consideration of solution conditions. The observed GI-EXAFS signal is not likely to originate from solution species or homogenous Cr precipitates for the following reasons. Solutions were undersaturated with respect to any known hydroxide, carbonate, or basic salt (e.g., Smith & Martell, 1976). The formation of any unknown mixed Fe/Cr precipitate appears to be unlikely based on the insignificant dissolution of iron during the course of the experiment. The total dissolved iron is estimated to be far below 10^{-13} mol (Cornell & Schwertmann, 1996), and corresponds to less than 1% of the total amount of 'sorbed' chromium. In addition, mixed precipitates were not observed in systems with higher susceptibility to this kind of precipitation phenomenon (e.g., Charlet & Manceau, 1992). Furthermore, the nucleation of a precipitate would be expected to take place in a 3-D fashion resulting in more pronounced more distant metal-metal features than we observed (critical nucleation size generally >10Å). Finally, the existence of dissolved multimers in solution can be ruled out based on kinetic and structural arguments (Rotzinger et al., 1986).

The existence of Cr at the hematite-water interface in multinuclear complexes even at a surface coverage of <0.1 monolayer was not anticipated based on the findings of earlier

EXAFS studies of metal ion surface complexation as a function of metal loading. For example, the EXAFS studies of Chisholm-Brause et al. (1990) and Towle et al. (1995) found evidence for mononuclear complexes of Co(II) at the lowest surface coverages examined (~0.05 μM/m^2), with multinuclear complexes or precipitates forming at higher surface coverages. Nevertheless, our finding of multinuclear Cr surface complexes is consistent with previous studies (Charlet & Manceau, 1992; Eggleston & Stumm, 1993).

4. Summary and Conclusions

Small, predominately two-dimensional Cr(III) clusters were found even at extremely low surface coverages and under-saturated solution conditions on (0001) hematite surfaces. The reduction of Cr(VI) to Cr(III) by partially reduced hematite surfaces leads to similar surface species as found after Cr(III) sorption.

This study revealed the presence of multinuclear Cr surface species rather than isolated mononuclear surface complexes on the hematite (0001) surface. Such multinuclear complexes should have a distinctively different reactivity than isolated monomer species, including a higher threshold for desorption. The finding of multinuclear surface complexes emphasizes the need for an improved, molecular-level conceptualization of reactions occurring at the solid-aqueous solution interface.

References

Charlet, L. & Manceau, A. A. (1992). J. Coll. Interf. Sci. 148, 443-458.
Citrin, P. H. (1985). Phys. Rev. B 31, 700-721
Chisholm-Brause, C. J., O'Day, P. A., Brown, G. E., Jr. & Parks, G. A. (1990). Nature 348, 528-531.
Cornell, R. M. & Schwertmann, U. (1996). The Iron Oxides: Structure, Properties, Reactions, Occurrence and Uses, Weinheim: VCH.
Dzombak, D. A. & Morel, F. M. M. (1990). Surface Complexation Modeling: Hydrous Ferric Oxide, New York: Wiley-Interscience.
Eggleston, C. M. & Stumm, W. (1993). Geochim. Cosmochim. Acta 57, 4843-4850.
George, G. N. & Pickering, I. J. (1995). EXAFS-PAK. Technical Report, Stanford Synchrotron Radiation Laboratory, Stanford, CA.
Kendelewicz, T., Liu, P., Doyle, C. S., Brown, G. E., Jr., Nelson, E. J. & Chambers, S. A. (1998). Surf. Sci., in press.
Kim, Y. J., Gao, Y. & Chambers, S. A. (1997). Surf. Sci. 371, 358-370.
Peterson, M. L., Brown, G. E., Jr. & Parks, G. A. (1996). Coll. Surf. A 107, 77-88.
Peterson, M. L., Brown, G. E., Jr., Parks, G. A. & Stein, C. L. (1997a). Geochim. Cosmochim. Acta 57, 3399-3412.
Peterson, M. L., White, A. F., Brown, G. E., Jr. & Parks, G. A. (1997b). Environ. Sci. Technol. 31, 1573-1576.
Rehr, J. J., Albers, R. C. & Zabinski, S. I. (1992). Phys. Rev. Lett. 69, 3397-3400.
Rotzinger, F. P., Stuenzi, H. & Marty, W. (1986). Inorg. Chem. 25, 489-495.
Smith, R. M. & Martell, A. E. (1976). Critical Stability Constants. New York: Plenum Press.
Stumm, W. & Morgan, J. J. (1996). Aquatic Chemistry, 3rd ed. New York: Wiley-Interscience.
Towle, S. N., Bargar, J. R., Brown, G. E., Jr., Parks, G. A. & Troy W., Jr. (1995). Mater. Res. Soc. Symp. Proc. 357, 23-28.